Deficiency in hepatic ATP-citrate lyase affects VLDL-triglyceride mobilization and liver fatty acid composition in mice[S]

Qiong Wang,[1,2] Shoufeng Li,[1] Lei Jiang,[3] Yunhua Zhou, Zi Li, Mengle Shao, Wenjun Li, and Yong Liu[4]

Key Laboratory of Nutrition and Metabolism, Institute for Nutritional Sciences, Shanghai Institutes for Biological Sciences; Graduate School of the Chinese Academy of Sciences, Chinese Academy of Sciences (CAS), Shanghai, China

Abstract **ATP-citrate lyase (ACL) is a key lipogenic enzyme that converts citrate in the cytoplasm to acetyl-CoA, the initial precursor that yields malonyl-CoA for fatty acid biosynthesis. As cytosolic citrate is derived from the tricarboxylic acid cycle in the mitochondrion, ACL catalyzes a critical reaction linking cellular glucose catabolism and lipid synthesis. To investigate the metabolic action of ACL in lipid homeostasis, we specifically knocked down hepatic ACL expression by adenovirus-mediated RNA interference in mice maintained on a low-fat or high-fat diet. Hepatic ACL abrogation markedly reduced the liver abundance of both acetyl-CoA and malonyl-CoA regardless of dietary fat intake, which was paralleled with decreases in circulating levels of triglycerides and free fatty acids. Moreover, hepatic ACL knockdown resulted in diet-dependent changes in the expression of other lipogenic enzymes, accompanied by altered fatty acid compositions in the liver. Interestingly, ACL deficiency led to reduced serum VLDL-triglyceride levels but increased hepatic triglyceride content, resulting at least partially from decreased hepatic secretion of VLDL-containing apolipoprotein B-48. Together, these results demonstrate that hepatic ACL suppression exerts profound effects on triglyceride mobilization as well as fatty acid compositions in the liver, suggesting an important role for ACL in lipid metabolism.**—Wang, Q., S. Li, L. Jiang, Y. Zhou, Z. Li, M. Shao, W. Li, and Y. Liu. **Deficiency in hepatic ATP-citrate lyase affects VLDL-triglyceride mobilization and liver fatty acid composition in mice.** ***J. Lipid Res.*** **2010.** 51: **2516–2526.**

Supplementary key words hypotriglyceridemia • apolipoprotein B • diet-induced obesity

As a major site for energy storage, processing, and conversion, the liver is a critical organ in the homeostatic control of both carbohydrate and lipid metabolism in mammals. De novo lipogenesis, which consists of a series of sequential reactions catalyzed by lipogenic enzymes (1), is a key metabolic process in the liver that contributes to the coordinate partitioning of energy fuels in response to changes in body's nutritional cues. Fatty acid biosynthesis is initiated in the cytosol with the generation of acetyl-CoA (CoA) from citrate that is transported out of the mitochondrion via the tricarboxylate transport system (2). ATP-citrate lyase (ACL) (3) catalyzes this crucial step that links cellular glucose catabolism and fatty acid synthesis. Further conversion of acetyl-CoA to malonyl-CoA is catalyzed by acetyl-CoA carboxylase (ACC), which is the rate-limiting reaction in de novo fatty acid synthesis (4). Fatty acids are synthesized from malonyl-CoA through processes catalyzed by fatty acid synthase (FAS), long-chain elongase (ELOVL-6), and stearoyl-CoA desaturase-1 (SCD1) (5). Saturated or unsaturated fatty acids are utilized to produce triglycerides (TG) by glycerol-3-phosphate acyltransferase (GPAT) and diacylglycerol acyltransferase (DGAT), which can be mobilized and transported from the liver primarily in the form of VLDL into circulation (6).

This work was supported by the National Natural Science Foundation Grants 30988002, 30830033, and 90713027; by the Ministry of Science and Technology 973 Programs 2006CB503900 and 2007CB947100; by the Chinese Academy of Sciences Knowledge Innovation Programs KSCX1-YW-02 and KSCX2-YW-R-115, CS Program SIBS2008006, and CAS/SAFEA International Partnership Program; and by the Science and Technology Commission of Shanghai Municipality (No. 10XD1406400 to Y.L. and W.L.).

Manuscript received 25 October 2009 and in revised form 20 May 2010.

Published, JLR Papers in Press, May 20, 2010
DOI 10.1194/jlr.M003335

Abbreviations: ACC, acetyl-coenzyme A carboxylase; AceCS, acetyl-CoA synthetase; ACL, ATP-citrate lyase; Apo, apolipoprotein; FPLC, fast-protein liquid chromatography; HFD, high-fat diet; LFD, low-fat diet; LPL, lipoprotein lipase; SCD1, stearoyl-CoA desaturase 1; TG, triglyceride.

[1] Q. Wang and S. Li contributed equally to this work.

[2] Present address of Q. Wang: Touchstone Diabetes Center, Department of Internal Medicine, University of Texas Southwestern Medical Center, Dallas, TX.

[3] Present address of L. Jiang: Simmons Comprehensive Cancer Center, University of Texas Southwestern Medical Center, Dallas, TX.

[4] To whom correspondence should be addressed:
e-mail: liuy@sibs.ac.cn

[S] The online version of this article (available at http://www.jlr.org) contains supplementary data in the form of three figures.

Lipogenesis is a metabolic pathway that is coordinately regulated in responding to nutritional and hormonal stimuli. Dysregulated lipogenesis has been shown to contribute significantly to the occurrence of dyslipidemia and the progression of metabolic disorders (7–9). Although gene expression profiling studies in animal models have revealed obesity-associated dysregulation of lipogenic gene expression (10–13), the metabolic contribution in the liver of each individual lipogenic enzyme to lipid metabolism as well as whole-body energy homeostasis has not been fully addressed until recently (11, 14–20). For instance, it has been reported that liver-specific ACC1 knockout mice (LACC1KO), while showing decreased liver TG contents with unchanged serum TG levels under fed states, exhibit no alterations in glucose homeostasis but much lower accumulation of lipids in the liver when fed a fat-free diet for 28 days (21). Unlike LACC1KO mice, however, mice with ablation of FAS in the liver (FASKOL mice) fed a zero-fat diet for 28 days develop fatty liver and hypoglycemia with decreased ketone bodies (22). Whereas hepatic FAS ablation dramatically increases malonyl-CoA accumulation, ACC1 deficiency in the liver results in decreased production of malonyl-CoA, which is known as a crucial physiological inhibitor of lipid β-oxidation (21). In addition, liver-specific knockout of SCD-1 (LSCD1KO mice), which catalyzes the production of various unsaturated fatty acids, leads to protection of mice from adiposity and hepatic steatosis induced by a high-sucrose, very low-fat diet, but not by a high-fat diet (19). These studies all point to distinct metabolic consequences resulting from deficiency in each of the lipogenic enzymes, especially under different nutritional conditions.

As a key lipogenic enzyme, ACL is most abundantly expressed in the liver and white adipose tissues, while exhibiting low expression levels in the brain, heart, small intestine, and muscles (23). Global ACL ablation in mice has been shown to result in embryonic lethality, indicative of its essential role in embryonic development (24). With respect to ACL's cellular functions, several groups have recently demonstrated that knockdown of ACL expression can suppress the proliferation and survival of several tumor cell lines with high glycolytic activities, suggesting that ACL, as an essential molecule in utilizing carbohydrates to provide carbon sources for cellular lipid synthesis required for tumor cell growth, represents a promising target for developing antitumor therapeutics (25–27). Animal studies have also shown that pharmacological inhibition of ACL at the whole-body level results in hypolipidemia and leads to prevention of high-fat diet-induced weight gain and hyperlipidemia (28–30). Similar to other lipogenic enzymes, ACL is also nutritionally regulated in response to changes in body's energy status. It has been reported that hepatic ACL in rodents displays relatively low expression levels in the state of starvation, whereas it is dramatically upregulated upon refeeding, with most prominent induction seen when fed a high-carbohydrate, low-fat diet (31). Currently, it remains largely unclear to what extent hepatic ACL affects lipid metabolism in response to changes in body's nutritional states.

Previously we have demonstrated that ACL in the liver, which is found to be markedly suppressed in mice fed a high-fat diet (13), acts as a critical component in mediating leptin's metabolic functions in regulating lipid and glucose metabolism (32). In leptin receptor-deficient *db/db* mice where hepatic ACL is abnormally elevated, targeted suppression of ACL in the liver can prominently correct obesity-associated fatty liver and hyperglycemia (32). To further understand the physiological contribution of hepatic ACL to lipid homeostasis, we investigated the metabolic consequences of hepatic ACL deficiency in mice under different nutritional conditions.

EXPERIMENTAL PROCEDURES

Animal studies

C57BL/6 male mice (Shanghai Laboratory Animal Co. Ltd) were housed in laboratory cages at a temperature of 23 ± 3°C and a humidity of 35 ± 5% under a 12 h dark/light cycle (lights on at 6:30 a.m.) in accredited animal facilities at the Shanghai Institutes for Biological Sciences, CAS. Mice maintained on normal chow diet were infected with the adenoviruses and then fed ad libitum a low-fat diet (LFD, 10 kcal% fat) or high-fat diet (HFD, 60 kcal% fat) (Research Diets, Inc., New Brunswick, NJ). Total body fat content was measured by nuclear magnetic resonance (NMR) using the Minispec Mq7.5 (Bruker, Germany). Oxygen consumption and motility were determined for mice fed ad libitum in the comprehensive laboratory animal monitoring system (CLAMS, Columbus Instruments) according to the manufacturers' instructions. After acclimation to the system for 6 h, O_2 and CO_2 were measured for the following 24 h (through a 12 h light/dark cycle). Oxygen consumption was normalized to lean mass, and respiratory exchange ratio (RER) was calculated. Voluntary activity was determined by monitoring the X-axis beam breaks every 15 min. All animals were euthanized under anesthetic conditions. Livers were snap-frozen in liquid nitrogen immediately after resection and stored at −80°C. All experimental procedures and protocols were approved by the Institutional Animal Care and Use Committee of the Institute for Nutritional Sciences, CAS.

Generation and administration of recombinant adenoviruses

Recombinant adenoviruses Ad-shACL and Ad-shLacZ, which express shRNAs directed against ACL and LacZ genes, respectively, were generated using the BLOCK-iT™ Adenoviral RNAi Expression System (Invitrogen, Carlsbad, CA) as previously described (32). The two adenoviruses used for ACL knockdown contain the following target sequences: 5′-GCTGAATACCGAGGACATTAA-3′ for Ad-shACL1# and 5′-GCATTAAGCCTGGATGCTTTA-3′ for Ad-shACL4#, respectively. High-titer stocks of amplified recombinant adenoviruses were purified, and viral titers were determined by the tissue culture infectious dose 50 (TCID50) method. Viruses were diluted in PBS and administration was performed through tail-vein injection at approximately 5×10^8 pfu/mouse.

Blood and liver measurements

Hepatic triglyceride levels were measured by using 40–50 mg of liver tissue homogenized in 1.5 ml of a mixture of $CHCl_3$-CH_3OH (2:1, v/v), followed by shaking at room temperature for 2 h. After addition of 0.5 ml of 0.1 M NaCl, the suspension was centrifuged at 3,700 rpm for 10 min, and the lower organic phase

was transferred and air-dried in a chemical hood overnight. The residual liquid was resuspended in 400 μl of 1% Triton X-100 in absolute ethanol, and the concentrations of triglyceride and cholesterol were analyzed using the commercial kits for blood measurements. Blood glucose was measured by a glucometer (FreeStyle, Alameda, CA). Serum and liver levels of triglycerides, FFA, β-hydroxybutyrate, and alanine transaminase (ALT) were determined using the Serum Triglyceride Determination Kit (Sigma, St. Louis, MO), FFA Half-micro Test (Roche Applied Science, Penzberg, Germany), β-Hydroxybutyrate LiquiColor (Stanbio, Boerne, TX) and Alanine Transaminase Determination Kit (ShenSuoYouFu, Shanghai, China), respectively.

Determination of ACL activity

ACL enzyme activity was determined using the malate dehydrogenase (MDH)-coupled method as described (32). Briefly, liver extracts were incubated in the reaction buffer containing 20 mM citrate, 10 mM $MgCl_2$, 10 mM DTT, 0.5 U/ml malic dehydrogenase, 0.33 mM CoASH, 0.14 mM NADH, and 100 mM Tris (pH 8.7), with or without 5 mM ATP. The yield of oxaloacetate generated by ACL catalysis was measured as the change in absorbance at 340 nm resulting from the consumption of NADH by the MDH-catalyzed reaction at 37°C. After subtracting the background changes, relative ACL activities were calculated by normalization to the total protein abundance of the extracts.

Antibodies and Western immunoblot analysis

ACL and ACC antibodies were from Cell Signaling, Boston, MA; Monoclonal FAS antibody was purchased from BD Biosciences, San Jose, CA; GAPDH antibody was from KangChen, Shanghai, China; apoB antibody was from RayBiotech, Norcross, GA. For Western immunoblot analysis, tissue extracts were prepared by lysis with CelLytic™ MT (Sigma, St. Louis, MO) and centrifuged for 20 min at 20,000 *g* to remove the debris. Proteins (20–40 μg) from liver extracts or fast-protein liquid chromatography (FPLC) fractionation samples were separated by SDS-PAGE and transferred to PVDF filter membrane (Amersham Biosciences, Piscataway, NJ), which was subsequently subjected to immunoblotting with the desired antibodies.

Real-time quantitative RT-PCR

Total liver RNA was isolated using TRIzol reagent (Invitrogen, Carlsbad, CA). After treatment with RNase-free DNase I (Roche Applied Science, Penzberg, Germany), first-strand cDNA was synthesized with M-MLV reverse transcriptase and random hexamer primers (Invitrogen). Real-time quantitative PCR was performed with the SYBR Green PCR system (Applied Biosystems, Foster City, CA), using GAPDH as an internal control for normalization. Primers used for each target gene were as follows: ACL, 5′-TGGATGCCACAGCTGACTAC-3′ and 5′-GGTTCAGCAAGGTCAGCTTC-3′; ACC1, 5′-TGAATCTCACGCGCCTACTATG-3′ and 5′-ATGACCCTGTTGCCTCCAAAC-3′;FAS,5′AAGTTGCCCGAGTCAGAGAA-3′ and 5′-CGTCGAACTTGGAGAGATCC-3′; SCD1, 5′-GCGATACACTCTGGTGCTCA-3′ and 5′-CCCAGGGAAACCAGGATATT-3′; AceCS1, 5′-CGGACAGAGGGTGGCTATTA-3′ and 5′-AGGGTACCCAATGACAGCAG-3′;AceCS2,5′-ATCCCCACATACCCAGATGA-3′ and 5′-GGTGCCGTGTAGAACTTGGT-3′; DGAT1, 5′-GTGTGTGGTGATGCTGATCC-3′ and 5′-GATGCAATAATCACGCATGG-3′; DGAT2, 5′-AGGCCCTATTTGGCTACGTT-3′ and 5′-GATGCCTCCAGACATCAGGT-3′; ELOVL6, 5′-TGCCATGTTCATCACCTTGT-3′ and 5′-TGCTGCATCCAGTTGAAGAC-3′; apoB, 5′-CAAGCACCTCCGAAAGTA-3′ and 5′-CACGGTATCCAGGAACAA-3′; apobec1, 5′-CGGGAGCTTCGGAAAGAGA-3′ and 5′-TCAACGTGGTTGCTGGTGTT-3.

Quantification of acetyl-CoA and malonyl-CoA

Homogenized liver tissues (20–25 mg) were added to the extraction solution (5% 5-sulfosalicylic acid containing 50 μM 1,4-dithioerythritol) at a ratio of 1:10 (w/v). After centrifugation at 14,000 *g* for 15 min at 4°C, the tissue homogenates were subjected to analysis by HPLC (Agilent 1200) and tandem mass spectrometry using negative-ion mode electrospray ionization with a 4000 Q-Trap system (Applied Biosystems, Foster City, CA) as previously described (32). The molecular ion peaks $[M\text{-}H]^-$ for acetyl-CoA, malonyl-CoA, and the internal standard n-propionyl-CoA were at *m/z* 808.3, 852.3 and 822.4, and their multiple reaction monitoring (MRM)-selected ions were 808.3/408.2, 852.3/408.2 and 822.4/408.3, respectively.

Quantitative profiling of hepatic fatty acids

A modified Bligh and Dyer protocol was used to extract total lipids from the liver homogenates with a chloroform-methanol-water (2:1:0.8) mixture (33). Freshly prepared 1,2-diheptadecanoyl-sn-glycero-phosphocholine (17:0) (Avanti Polar Lipids, Inc., AL) was added as an internal standard before homogenization. The extracts were saponificated using sodium hydroxide, followed by esterification with boron-trifluoride (BF3) (Sigma) in methanol to generate fatty acid methyl esters (FAME). Purified FAMEs were subsequently dissolved in heptane and stored in −20°C for further analysis.

Total FAMEs were analyzed by gas chromatography-mass spectrometry (GC-MS) with a flame ionization detector (Agilent 5975B Inert XL MSD with 6890N GC; SP-2560 capillary column: 100 m × 0.25 mm I.D. × 0.20 μm film, Supelco, Inc., PA). Quantitative profiles were calculated using methyl-17:0 as the internal standard and an equal weight FAME mixture 68A (Nuchek Prep, Elysian, MN) as the response factor for each FAME. The amount of each fatty acid was calculated as relative to the wet weight of liver.

Hepatic triglyceride secretion rate and lipoprotein fractionation

Hepatic triglyceride secretion rates were determined by measuring the increases in serum triglycerides after inhibition of lipoprotein lipase via tail-vein injection of tyloxapol (Sigma-Aldrich, St. Louis, MO) at 600 mg/kg, a dose that was supposed to completely inhibit triglyceride clearance during VLDL secretion experiments (34). Serum samples were taken from the tail vein every h for triglyceride analysis.

For lipoprotein fractionation analysis, equal volumes of serum samples were pooled from mice for each group in the fed states (a total volume of 400 μl). Lipoproteins were fractionated using a Superose 6 10/300 GL FPLC column (Amersham Biosciences, Piscataway, NJ). Fractions (500 μl) were collected and used for triglyceride and cholesterol analysis. For detection of apoB100 and apoB48, aliquots of the FPLC elution fractions were mixed with protein loading buffer and heated at 95°C for 6 min before Western immunoblot analysis.

Analysis of apoB mRNA editing

For the measurement of C to U editing efficiency of apoB mRNA in the liver, a gel-purified 537-bp RT-PCR product harboring the editing site was subjected to direct sequencing. The primers used for PCR amplification of the editing region of apoB mRNA were: 5′-GCCCTGAGCAGACTTCCT-3′ and 5′-AATAGCGTCCATCTGTCG-3′. Editing efficiency was determined based on the T/C nucleotide signal ratio from the sequencing eletropherograms.

Histology

Liver tissue specimens were fixed in 10% neutral buffered formalin, and then paraffin-embedded sections were subjected to standard hematoxylin-eosin (H and E) staining.

Statistical analysis

Data are presented as means ± SEM. Differences were analyzed by unpaired two-tailed *t*-test between two groups or otherwise by one-way ANOVA.

RESULTS

Hepatic ACL suppression results in hypotriglyceridemia with elevated liver triglyceride contents

Previously we found that targeted suppression of dysregulated ACL in the liver of *db/db* mice dramatically reduced lipogenesis and led to markedly decreased levels of hepatic but not serum triglycerides (32). To further investigate the physiological importance of hepatic ACL in lipid homeostasis, we took the RNAi approach using two recombinant adenoviruses (Ad-shACL1# and 4#) that expressed shRNAs directed against two different coding regions of ACL. First we tested the effects of ACL knockdown in C57BL/6 mice maintained on a low-fat diet (10 kcal% fat). At 23 days post infection, both Ad-shACL1# and 4# efficiently knocked down the expression of ACL protein (supplementary Fig. I-A), resulting in a ~77% reduction in the hepatic ACL enzyme activity compared with mice infected with the control virus Ad-shLacZ (supplementary Fig. I-B). In contrast to our observations in *db/db* mice (32), hepatic ACL suppression by both viruses led to marked reductions in the serum levels of TG (Ad-shACL1# by ~52% and Ad-shACL4# by ~44%; supplementary Fig. I-C) but significant elevations in hepatic TG contents (Ad-shACL1# by 140% and Ad-shACL4# by 70%; supplementary Fig. I-D). These data indicate a direct connection of ACL to liver TG storage and mobilization under normal physiological conditions, ruling out possible off-target effects by the two knockdown adenoviruses. Therefore, we used Ad-shACL1# for subsequent experiments to examine the metabolic consequences of hepatic ACL deficiency under different conditions of dietary fat intake.

Diet-dependent effects of hepatic ACL knockdown on the expression of ACC and FAS and the production of lipogenic precursors

We next sought to determine the metabolic effects of targeted suppression of ACL on lipid metabolism under different nutritional states. Male C57BL/6 mice at 8 weeks of age were infected and maintained on an LFD versus HFD (60 kcal% fat). At 25 days post infection, Ad-shACL1# (indicated as Ad-shACL throughout the subsequent experiments) did not cause significant increases in functional liver damage or inflammation relative to Ad-shLacZ control virus, as evaluated by the serum levels of ALT (**Table 1**). Ad-shACL effectively diminished ACL protein expression as well as ACL enzyme activity (by >85% for LFD-fed mice and by >88% for HFD-fed mice) in the livers of both LFD- and HFD-fed mice (**Fig. 1A**, B). Curiously, in LFD-fed mice, hepatic ACL knockdown led to marked increases in the protein expression levels of ACC and FAS. By contrast and consistent with previously reported observations (13), ACL, ACC, and FAS were prominently suppressed in HFD-fed mice infected with Ad-shLacZ control virus. Further knockdown of ACL in HFD-fed mice led to significantly decreased FAS expression but unaltered expression of ACC (Fig. 1A). Therefore, hepatic ACL abrogation resulted in distinct diet-dependent alterations in the expression of other downstream lipogenic enzymes.

To examine whether ACL deficiency exerts diet-dependent effects on the production of precursor molecules for fatty acid synthesis, we measured the hepatic contents of both acetyl-CoA and malonyl-CoA by LC-MS-MS. As a result of HFD-induced suppression of hepatic ACL expression and activity (>70% decrease in ACL enzyme activities; Fig. 1B), a significant reduction in acetyl-CoA was observed in Ad-shLacZ-infected HFD-fed mice (Fig. 1C). Interestingly, in comparison with that of Ad-shLacZ-infected control mice, hepatic ACL knockdown resulted in ~25% reduction of the hepatic acetyl-CoA levels in Ad-shACL-infected mice fed LFD or HFD (Fig. 1C), although >85% decrease in ACL enzyme activities were observed (Fig. 1B). This indicates the

TABLE 1. Physiologic data and serum measurement of Ad-shLacZ- or Ad-shACL-infected mice fed LFD versus HFD

	LFD		HFD	
	Ad-shLacZ	Ad-shACL	Ad-shLacZ	Ad-shACL
Body weight (g)	21.7 ± 0.9	21.9 ± 1.1	23.2 ± 0.8	22.9 ± 0.8
Food intake (g/day)	2.87 ± 0.14	2.95 ± 0.16	2.32 ± 0.06	2.25 ± 0.15
Fat mass (g)	1.21 ± 0.23	1.03 ± 0.23	1.84 ± 0.61	1.85 ± 0.68
Lean mass (g)	18.86 ± 1.10	19.00 ± 1.30	19.73 ± 1.39	19.89 ± 0.94
Liver weight (g)	1.33 ± 0.13	1.41 ± 0.15	1.23 ± 0.22	1.16 ± 0.03
Epididymal fat weight (g)	0.280 ± 0.070	0.238 ± 0.036	0.315 ± 0.078	0.316 ± 0.054
Serum FFA (mM)	0.56 ± 0.06	0.39 ± 0.03[a]	0.64 ± 0.03	0.47 ± 0.04[a]
Serum triglyceride (mg/dl)	24.84 ± 2.83	13.49 ± 1.42[a]	35.17 ± 3.34	20.66 ± 3.27[b]
Serum cholesterol (mg/dl)	77.2 ± 2.8	93.2 ± 2.3[a]	109.4 ± 6.0	113.2 ± 2.6
Fasting glucose (mg/dl)	123.4 ± 22.1	112.7 ± 20.6	141.9 ± 45.5	130.0 ± 12.7
β-hydroxybutyrate (mM)	0.74 ± 0.34	0.72 ± 0.37	0.80 ± 0.29	1.68 ± 0.53[a]
ALT (U/l)	72.5 ± 10.1	57.2 ± 2.4	61.1 ± 9.1	91.7 ± 9.8

All data are from 8-week-old male C57BL/6J mice (n = 7–8 per group) infected for 25 days. Values are shown as means ± SEM. Abbreviations: ALT, alanine transaminase; HFD, high-fat diet; LFD, low-fat diet.

[a] $P < 0.05$ and versus Ad-shLacZ-infected control mice fed the same diet by ANOVA.

[b] $P < 0.01$ versus Ad-shLacZ-infected control mice fed the same diet by ANOVA.

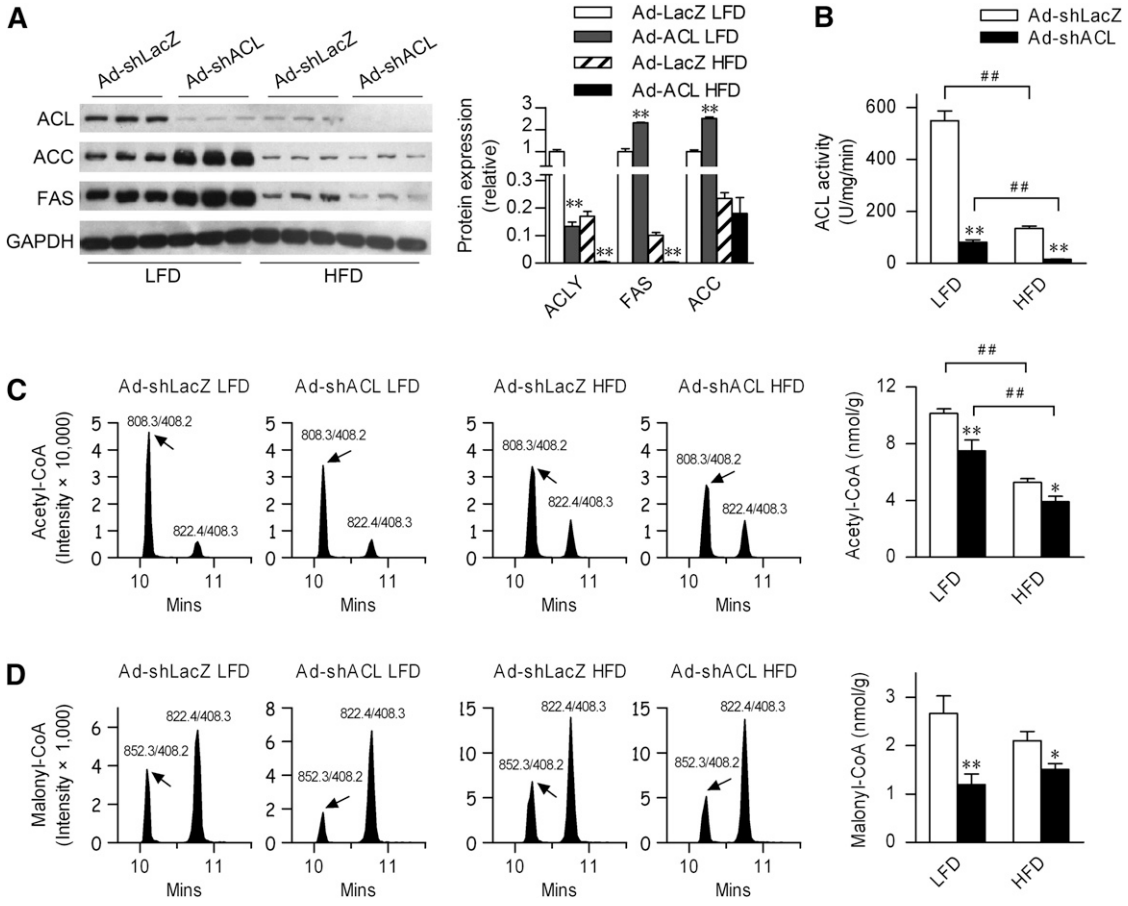

Fig. 1. Effects of hepatic ACL knockdown on the expression of lipogenic enzymes and the production of lipogenic precursors in mice fed LFD versus HFD. Male C57BL/6J mice (n = 7–8/group) at 8 weeks of age were infected through tail-vein injection with the control adenovirus Ad-shLacZ or the targeting adenovirus Ad-shACL1# (Ad-shACL) and then maintained on LFD or HFD for 25 days. Animals were euthanized under the fed state. A: Western immunoblots showing ACL, ACC, and FAS protein levels from the liver extracts. Each lane represents pooled samples from 2–3 mice. The bar graph indicates the relative protein abundance as quantified by densitometry from the immunoblots after normalization to GAPDH. B: ACL enzyme activities were measured from the liver extracts. C and D: Determination of acetyl-CoA and malonyl-CoA levels from the liver extracts by LC-MS/MS using the ABI 4000 Q-Trap system. Shown are representative analyses by tandem mass spectrometry of (C) acetyl-CoA (ion pair at 808.3/408.2) and (D) malonyl-CoA (at 852.3/408.2) from each individual mouse infected with Ad-shLacZ versus Ad-shACL, with n-propionyl-CoA (at 822.4/408.3) used as an internal reference. The bar graphs indicate the average levels calculated according to their standard curves (n = 7–8/group). Data are shown as means ± SEM. $^{*}P < 0.05$ and $^{**}P < 0.01$ versus Ad-shLacZ-infected mice fed the same diet by ANOVA; $^{\#\#}P < 0.01$ versus LFD-fed mice infected with the same adenovirus by ANOVA. ACC, acetyl-coenzyme A carboxylase; ACL, ATP-citrate lyase; HFD, high-fat diet; LFD, low-fat diet.

likely involvement of other compensatory sources of hepatic acetyl-CoA production as a result of ACL deficiency. In addition, despite of distinct ACC expression patterns, ~50% and ~28% decreases in hepatic malonyl-CoA levels, respectively, were detected in LFD- and HFD-fed mice infected with Ad-shACL (Fig. 1D), indicating the likely presence of additional factors that influence ACC activities (e.g., ACC phosphorylation) under these conditions. These results suggest that hepatic ACL deficiency can affect the lipogenic program in a diet-dependent manner, and the resulting alterations in the production of lipogenic precursors as well as in downstream lipogenic enzymes may lead to changes in fatty acid compositions in the liver.

Hepatic ACL abrogation affects circulating TG levels and hepatic TG storage regardless of diet

We then examined the metabolic effects of hepatic ACL knockdown in the context of HFD-induced obesity and dyslipidemia. Compared with Ad-shLacZ-infected mice, comparable increases were observed in both body weight gain and fat mass accumulation in Ad-shACL-infected mice fed HFD for 25 days (Table 1), and no appreciable changes were found in their metabolic rate, respiratory exchange ratio (RER), or physical activities (supplementary Fig. II). Moreover, serum levels of glucose were not significantly altered in the fasted state. Therefore, in the settings of the moderate adiposity induced by short-term HFD feeding (25 days), ACL abrogation did not cause significant changes in diet-dependent fat mass accumulation or glucose metabolism. Interestingly, ACL knockdown caused significantly elevated ketone bodies (β-hydroxybutyrate) in the fasted state after HFD feeding (Table 1), possibly reflecting increased fatty acid β-oxidation caused by reduced malonyl-CoA. On the other hand, compared with Ad-shLacZ-infected mice, hepatic ACL knockdown resulted in similar decreases in serum TG levels (by ~42%;

Fig. 2A and Table 1) and FFA levels (by 25–30%; Fig. 2B and Table 1) in Ad-shACL-infected mice fed LFD or HFD, completely correcting HFD-induced hypertriglyceridemia. However, whether maintained on LFD or HFD, hepatic ACL knockdown resulted in significantly increased TG levels in the liver (by ~45% in LFD-fed mice and by ~29% in HFD-fed mice; Fig. 2C), even though Ad-shLacZ-infected mice fed HFD already had a ~50% elevation in hepatic TG content relative to LFD-fed mice. Histological examination of liver sections revealed that in HFD-fed mice, hepatic ACL deficiency resulted in obvious appearance of lipid droplets (Fig. 2D). Thus, ACL knockdown in the liver exerted a prominent hypolipidemic effect independent of dietary fat intake that might result from decreased hepatic output or increased uptake of TG by the liver.

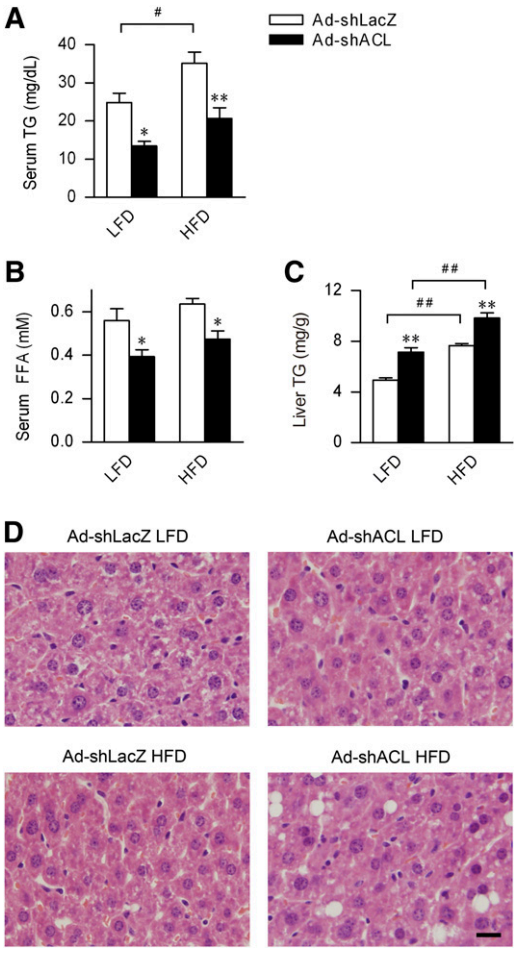

Fig. 2. Abrogation of hepatic ACL reduces circulating triglyceride levels but increases liver triglyceride contents. Measurements were done for adenovirus-infected mice fed LFD or HFD for 25 days, using samples collected under the fed state. A–C: Serum levels of (A) TG and (B) FFA and (C) liver TG contents were determined for mice infected with Ad-shLacZ or Ad-shACL (n = 7–8/group). Data are shown as means ± SEM. $^{*}P < 0.05$ and $^{**}P < 0.01$ versus Ad-shLacZ-infected mice fed the same diet; $^{\#}P < 0.05$, $^{\#\#}P < 0.01$ versus LFD-fed mice infected with the same adenovirus by ANOVA. D: Representative images of H and E staining of liver sections from mice of the indicated group (n = 5/group). Original magnification 10×. The bar indicates 0.5 mm. ACL, ATP-citrate lyase; H and E, hematoxylin-eosin; HFD, high-fat diet; LFD, low-fat diet; TG, triglyceride.

Knockdown of hepatic ACL reduces the circulating levels of VLDL-containing apolipoprotein B48

Fatty acids are transported from the liver to adipose tissues and other sites in the form of VLDL in circulation, and the major lipid constituents of VLDL are triglycerides (6). To determine whether decreased serum TG levels in ACL knockdown mice reflect reduced amounts of VLDL particles, we measured the TG contents from fractionated serum lipoproteins. In contrast to the unaltered levels of cholesterol associated with HDL, marked reductions in the TG contents (by ~47% in LFD-fed mice and ~57% in HFD-fed mice) were detected from the serum VLDL fractions from Ad-shACL-infected mice compared with Ad-shLacZ-infected control mice, either fed LFD or HFD (**Fig. 3A**, B). Moreover, decreased levels of TG associated with intermediate-density lipoprotein or low-density lipoprotein (IDL/LDL) were also observed (by ~38% and ~16% in LFD- and HFD-fed mice, respectively), presumably stemming from reductions in VLDL-TG (Fig. 3A). These data further indicate the presence of defective production of VLDL as a result of hepatic ACL deficiency.

As the major structural component of VLDL, two forms of apolipoprotein B, apoB100 and apoB48, exist as the products of a single gene with the same N-terminal region, arising from a C to U RNA editing event that introduces a translational stop codon in the apoB RNA transcript (35, 36). To test whether ACL knockdown-induced serum VLDL-TG reductions were associated with alterations of a particular apoB protein component, we analyzed the FPLC-fractionated VLDL lipoprotein profiles from the serum of LFD-fed mice infected with Ad-shLacZ or Ad-shACL. Surprisingly, as shown by Western immunoblot analysis, marked decreases in the amount of apoB48 but not apoB100 were detected in Ad-shACL-infected mice compared with control mice (Fig. 3C), with obviously reduced apoB48/aopB100 ratios (by >50%) observed in major VLDL fractions. These data indicate that hepatic ACL deficiency caused a selective decrease in the abundance of apoB48-containing VLDL in the circulation.

Hepatic ACL deficiency reduces hepatic secretion of VLDL-containing apoB48

Given the fact that changes in the circulating VLDL-TG levels can reflect its altered clearance from circulation or the impact of its hepatic secretion, we next analyzed the rate of hepatic lipid export in LFD-fed mice treated with tyloxapol, an inhibitor of lipoprotein lipase which could block VLDL hydrolysis by the peripheral tissues, thereby permitting the measurement of hepatic VLDL-TG production. Indeed, ACL abrogation led to a 23% decrease in the rate of hepatic VLDL-TG production in Ad-shACL-infected mice fed LFD relative to Ad-shLacZ-treated control mice (**Fig. 4A**), suggesting that ACL deficiency leads to decreased TG output from the liver.

We next performed FPLC fractionation of lipoproteins in the serum from mice similarly treated with tyloxapol for 4 h. In parallel with marked reductions in VLDL-TG, apparently decreased abundance of apoB48 protein was detected in the VLDL fractions in Ad-shACL-infected mice

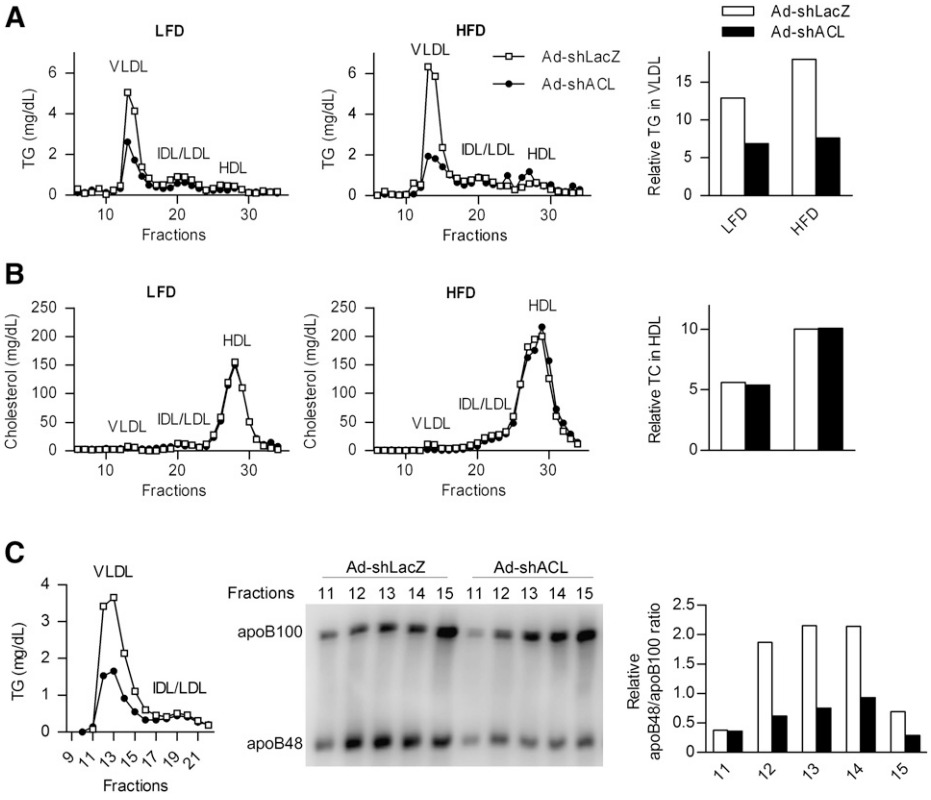

Fig. 3. Hepatic ACL deficiency results in reduced circulating VLDL containing apoB48. Lipoprotein profiles were determined using pooled serum samples (n = 5) by FPLC fractionation from adenovirus-infected mice fed LFD or HFD for 25 days (n = 7–8/group). A and B: TG and cholesterol concentrations were measured in each indicated fraction corresponding to VLDL, IDL/LDL, and HDL, respectively. The relative TG content in VLDL fractions and cholesterol content in HDL are also shown using the areas under curve from the FPLC profiles. C: Mice likewise infected were fed LFD for 28 days (n = 8). Serum samples were pooled (n = 5) and fractionated by FPLC, and the TG concentration in each fraction was measured (left). Equal volumes of the indicated VLDL fractions were subjected to Western immunoblot analysis using the apoB antibody. The bar graph indicates the relative apoB48/apoB100 ratio as quantified by densitometry from the immunoblots. ACL, ATP-citrate lyase; Apo, apolipoprotein; FPLC, fast-protein liquid chromatography; HFD, high-fat diet; LFD, low-fat diet; TG, triglyceride.

(Fig. 4B), while discernable increases were observed for the apoB100 protein whose abundance was much lower than that of apoB48 upon tyloxapol treatment. Similarly, prominently reduced apoB48:apoB100 ratios were seen from major VLDL fractions in ACL knockdown mice. Consistent with a selective decrease in the output of apoB48-containing VLDL, elevated apoB48 protein abundance was found in the liver of Ad-shACL-infected mice compared with that of Ad-shLacZ-infected control mice (Fig. 4C). To determine whether this increase in hepatic apoB48 protein level resulted primarily from reduced secretion or from changes in apoB RNA editing, we measured the efficiency of C to U editing by directly sequencing the RT-PCR products derived from apoB mRNA that harbor the editing site. In the liver of ACL knockdown mice, no significant alterations (supplementary Fig. III-A) were detected in the abundance of mRNAs encoding either apoB or apobec-1, the catalytic subunit within the multicomponent enzyme complex responsible for apoB RNA editing (36, 37). Curiously, a significant reduction in apoB RNA editing efficiency (by ~20% when expressed as the T/C ratio) was observed in the liver of Ad-shACL-infected mice (supplementary. Fig. III-B), which would presumably result in decreased hepatic translation production of apoB48 protein. Thus, these results further support that hepatic ACL knockdown caused decreased export of apoB48-containing VLDL from the liver, indicating a possible connection between ACL deficiency and the assembly or maturation of selective lipoprotein particles.

Impact of hepatic ACL deficiency upon lipogenic gene expression and fatty acid composition

To further determine the extent of the effects of hepatic ACL abrogation on lipid metabolism in the liver, we examined the expression profiles of genes related to triglyceride production as well as liver fatty acid composition. Given glucose as the major carbon source for acetyl-CoA production, the majority of cytosolic acetyl-CoA is thought to emanate from citrate by ACL-catalyzed reaction. In mammals, however, there are two acetyl-CoA synthetases (AceCS), AceCS1 and AceCS2, which are localized, respectively, in the cytoplasm and mitochondria to catalyze the formation of acetyl-CoA from acetate, thus offering alternative sources of acetyl-CoA. Consistent with the reduced

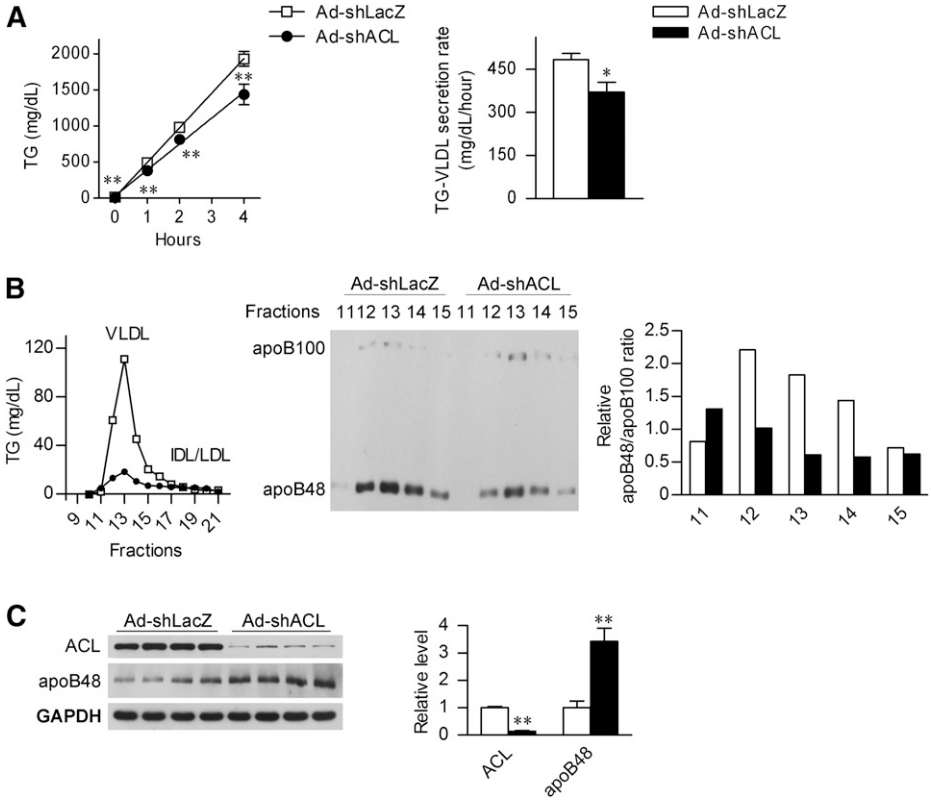

Fig. 4. Hepatic ACL deficiency suppresses the secretion of apoB48-containing VLDL. A: Male C57BL/6J mice at 8 weeks of age were infected with Ad-shLacZ or Ad-shACL and maintained on LFD for 18 days (n = 8/group). After a 4 h fast, tyloxapol was administered through tail-vein injection at 600 mg/kg to block the LPL activity. Blood triglycerides were measured at the time points as indicated, and the VLDL secretion rate was derived from the slope of the line using least squares regression. Data are shown as means ± SEM. $*P < 0.05$ and $**P < 0.01$ versus Ad-shLacZ-infected mice by t-Test. B: Mice likewise infected were treated with tyloxapol for 4 h, and serum samples were collected and pooled for FPLC fractionation analysis (n = 4). The TG concentration was determined from each of the indicated fractions, and equal volumes of the VLDL fractions were subjected to Western immunoblot analysis using the apoB antibody. The bar graph indicates the relative apoB48:apoB100 ratio after quantification by densitometry from the immunoblots. C: Western immunoblot analysis of the liver ACL and apoB48 protein abundance from the mice treated for 4 h with tyloxapol as in (B). Each lane represents analyzed sample from an individual mouse. The bar graphs indicate the relative abundance of ACL and apoB48 protein as quantified by densitometry from the immunoblots after normalization to GAPDH (n = 4/group). Data are shown as means ± SEM. $**P < 0.01$ versus Ad-shLacZ-infected mice. ACL, ATP-citrate lyase; Apo, apolipoprotein; FPLC, fast-protein liquid chromatography; HFD, high-fat diet; LFD, low-fat diet; TG, triglyceride.

protein levels observed (Fig. 1) in LFD- and HFD-fed mice infected by Ad-shACL, quantitative RT-PCR analysis showed markedly decreased ACL mRNA levels in the liver (**Fig. 5A**). Interestingly, while AceCS2, but not AceCS1, was downregulated by HFD feeding, hepatic ACL knockdown resulted in significant increases of the mRNA expression of AceCS2, but not AceCS1, in the liver of Ad-shACL-infected mice fed LFD and HFD (by ~73% and ~29%, respectively; Fig. 5A). This suggests that the mitochondrion-localized AceCS2 may be transcriptionally responsive to the cytoplasmic event of ACL deficiency. Somewhat surprisingly, the mRNA levels of FAS or ACC were not significantly altered in the liver of ACL knockdown mice, which contrasted with the changes observed in their protein levels (Fig. 1A), indicating that ACL deficiency did not influence their expression at the transcriptional level. Upon HFD feeding, the expression of FAS and ELOVL6 was significantly suppressed, and the most marked downregulation was observed for SCD1. Notably, ACL knockdown led to a ~38% increase in the mRNA expression of SCD1 in LFD-fed mice but a ~70% decrease in HFD-fed mice (Fig. 5A), suggesting that the SCD1 expression is under complex control in response to nutritional changes.

Given the observed impact of ACL deficiency on the expression patterns of genes related to lipid metabolism, we attempted to determine how ACL knockdown might alter the entire fatty acid composition in total liver lipids upon different dietary fat intake using GC-MS (Fig. 5B). This fatty acid profiling analysis revealed that HFD feeding did not elicit dramatic alterations in the fatty acids in high abundances (e.g., the saturated fatty acids palmitate and stearate) and caused merely slight increases in the fatty acid 18:2n6. However, in both Ad-shLacZ- and

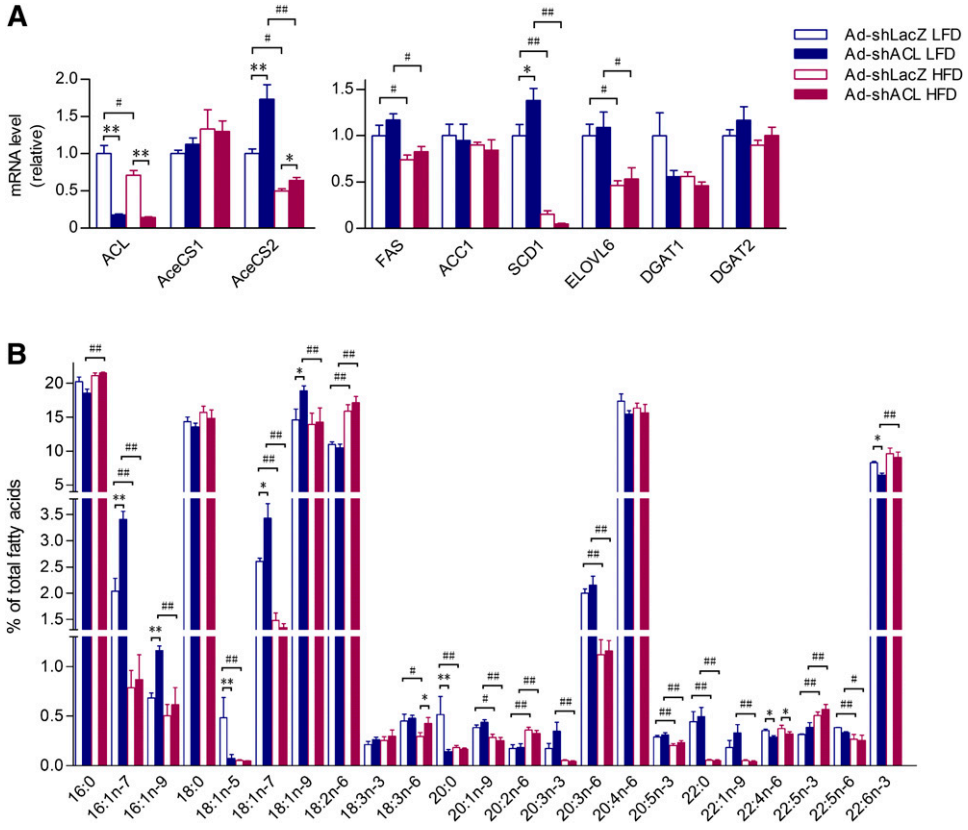

Fig. 5. Impact of ACL knockdown on the expression of genes related to TG metabolism and total hepatic fatty acid composition. Mice at 8 weeks of age were infected with Ad-shLacZ or Ad-shACL and fed LFD or HFD for 25 days. Liver RNAs or total fatty acids were prepared from mice under the fed state. A: The mRNA expression level was determined for each indicated gene involved in acetyl-CoA generation and TG synthesis by real-time quantitative RT-PCR and expressed as relative to that of the Ad-shLacZ-infected control group fed LFD (set as 1.0) with GAPDH used as the internal control. Data are shown as means ± SEM (n = 7–8/group). B: Profiling analysis by GC-MS of liver fatty acid species ranging from 16 to 22 carbons. The relative abundance of each indicated fatty acid is expressed as the percentage of the total fatty acids determined for each sample. Data are shown as means ± SEM (n = 5–6/group). $^{*}P < 0.05$ and $^{**}P < 0.01$ versus Ad-shLacZ-infected mice fed the same diet by ANOVA; $^{\#}P < 0.05$, $^{\#\#}P < 0.01$ versus LFD-fed mice infected with the same adenovirus by ANOVA. ACL, ATP-citrate lyase; GC-MS, gas-chromatography mass-spectroscopy; HFD, high-fat diet; LFD, low-fat diet; TG, triglyceride.

Ad-shACL-infected mice fed HFD, significant reductions were detected in the amount of monounsaturated fatty acids (MUFA) 16:1n7-palmitoleate and 18:1n7-oleate (Fig. 5B), possibly as a result of HFD-induced SCD1 suppression (Fig. 5A). Moreover, among other changes in low-abundance fatty acids, only in LFD-fed mice did hepatic ACL knockdown lead to significantly increased contents of MUFAs, most notably C16:1n7-palmitoleate (by 67%), C16:1n9-palmitoleate (by 70%), C18:1n7-oleate (by 32%) and C18:1n9-oleate (by 30%). Together, these results indicate that hepatic ACL deficiency can bring about profound effects on the fatty acid composition, particularly affecting the production of MUFAs in the liver.

DISCUSSION

This study aimed to explore the physiological actions of hepatic ACL in lipid homeostasis in response to nutritional changes using mice fed a low-fat diet versus a high-fat diet. We found that abrogation of hepatic ACL resulted in hypotriglyceridemia, even in the face of a high-fat diet challenge, with alterations in several aspects of lipid metabolism in the liver that ranged from fatty acid composition to triglyceride mobilization and VLDL secretion. These results reveal the metabolic importance of hepatic ACL in lipid homeostasis.

Previously we have shown that in *db/db* mice, a genetic obesity mouse model with hepatic steatosis and dyslipidemia, ACL expression is dramatically elevated in the liver; knockdown of the abnormally upregulated ACL leads to subsequent suppression of the key lipogenic regulator PPARγ as well as the entire lipogenic program, preventing the development of fatty liver but not hypertriglyceridemia (32). In contrast, here we observed different metabolic consequences resulting from hepatic ACL abrogation in normal mice, most notably hypotriglyceridemia along with increased hepatic TG content. Given the profound metabolic derangements caused by leptin receptor deficiency in *db/db* mice, it is conceivable that in the presence versus

absence of the functional leptin receptor, ACL abrogation could exert distinct effects on lipid metabolism through affecting different sets of crucial regulatory molecules, as exemplified by hepatic PPARγ, whose expression is prominently increased in *db/db* mice (32).

The lipogenic pathway is a highly regulated process that plays an important part in coordinating body's partitioning of energy fuels. Perturbation at different steps of lipogenic pathway brings about distinct metabolic phenotypes under different conditions of dietary fat intake, as demonstrated by the studies of mouse models with liver-specific knockout of ACC1 (21), FAS (22), or SCD1 (19). The results from the current study showed that ACL deficiency could influence the expression of downstream lipogenic genes in a diet-dependent fashion (e.g., triggering increased expression levels of ACC and FAS proteins as well as SCD1 mRNA when fed LFD). It is notable that, whether maintained on LFD or HFD, liver ACL deficiency resulted in lower amount of malonyl-CoA and increased TG storage in the liver, which is different from the metabolic phenotypes of hepatic ACC1 knockout mice exhibiting reduced malonyl-CoA levels but dramatically decreased accumulation of lipids in the liver when fed a fat-free diet. Of additional note, in the face of HFD feeding that led to suppressed expression of lipogenic enzymes including FAS, ACC, and SCD1 in the liver, ACL deficiency failed to trigger the induction of these lipogenic genes as seen when fed LFD. Whereas it is currently unclear what diet-dependent mechanisms are involved in mediating the distinct effects of ACL deficiency on the expression levels of these lipogenic enzymes, this may at least partially account for the observation that ACL knockdown caused extensive diet-responsive changes in the total fatty acid composition in the liver, particularly the levels of MUFAs, such as C16:1n7-palmitoleate, C16:1n9-palmitoleate, C18:1n7-oleate, and C18:1n9-oleate. The alterations in the fatty acid profiles could reflect part of the ACL deficiency-induced metabolomic changes, which could in turn influence not only lipid metabolism but also glucose homeostasis. For instance, it was recently reported that C16:1n7-palmitoleate could act as a so-called "lipokine" playing a key role in regulation of the lipogenic pathway and systemic glucose metabolism (38). On the other hand, we did not observe a significant impact of hepatic ACL suppression on HFD-induced accumulation of body fat mass or glucose metabolism during the relatively short period (25 days) of the adenoviral knockdown experiment. While this is consistent with our earlier findings (13) that the moderate adiposity levels were not associated with overt insulin resistance in mice upon short-term HFD feeding, it remains to be deciphered whether chronic deficiency in hepatic ACL can affect glucose homeostasis under long-term HFD feeding conditions.

Our results also showed that the hypotriglyceridemic effect of hepatic ACL deficiency might largely arise from decreased VLDL secretion, in parallel with increased TG content in the liver. This provides another example of the lipogenic enzyme in affecting hepatic VLDL secretion and triglyceride output, as it was documented that inhibition of the hepatic SCD1 activity could mediate the central glucose's action in downregulating triglyceride synthesis and VLDL secretion from the liver (34, 39). In addition, we observed that ACL knockdown caused marked reductions in the hepatic output of apoB48-containing VLDL molecules, accompanied by increased abundance of apoB48 protein in the liver. Interestingly, without influencing the levels of mRNA transcripts encoding apoB or apobec-1, ACL knockdown led to considerable reduction in apoB RNA editing. Given the existence of multiple regulatory factors involved in the assembly of a multiprotein editosome responsible for apoB RNA editing (40), how ACL deficiency influenced this editing process remains currently unknown. It is worth noting that a recent study demonstrated a crucial role of ACL in regulation of histone acetylation through controlling the nuclear levels of acetyl-CoA (41), linking cellular ACL activities to the metabolic control of histone acetylation and, consequently, gene expression programs. In this regard, ACL deficiency may exert a potential impact on the extent of protein acetylation modifications and thus the activation status of key metabolic regulators such as PGC1α and LXR (42–44). Therefore, it is not surprising that hepatic ACL suppression could have various effects on a range of lipid metabolism-related events from lipogenic gene expression, to apoB RNA editing, to VLDL secretion. While the detailed molecular nature of these ACL-dependent changes has yet to be further elucidated, our findings provide insights for fully understanding the metabolic importance of hepatic ACL in the face of changing nutritional conditions, especially in the maintenance of lipid homeostasis.

The authors thank Jun Shen for assistance with CLAMS.

REFERENCES

1. Wakil, S. J., J. K. Stoops, and V. C. Joshi. 1983. Fatty acid synthesis and its regulation. *Annu. Rev. Biochem.* **52:** 537–579.
2. Kaplan, R. S., J. A. Mayor, N. Johnston, and D. L. Oliveira. 1990. Purification and characterization of the reconstitutively active tricarboxylate transporter from rat liver mitochondria. *J. Biol. Chem.* **265:** 13379–13385.
3. Srere, P. A. 1959. The citrate cleavage enzyme. I. Distribution and purification. *J. Biol. Chem.* **234:** 2544–2547.
4. Thampy, K. G., and A. G. Koshy. 1991. Purification, characterization, and ontogeny of acetyl-CoA carboxylase isozyme of chick embryo brain. *J. Lipid Res.* **32:** 1667–1673.
5. Ntambi, J. M., and M. Miyazaki. 2003. Recent insights into stearoyl-CoA desaturase-1. *Curr. Opin. Lipidol.* **14:** 255–261.
6. Havel, R. J., and J. P. Kane. 1975. Quantification of triglyceride transport in blood plasma: a critical analysis. *Fed. Proc.* **34:** 2250–2257.
7. Lewis, G. F., A. Carpentier, K. Adeli, and A. Giacca. 2002. Disordered fat storage and mobilization in the pathogenesis of insulin resistance and type 2 diabetes. *Endocr. Rev.* **23:** 201–229.
8. Browning, J. D., and J. D. Horton. 2004. Molecular mediators of hepatic steatosis and liver injury. *J. Clin. Invest.* **114:** 147–152.
9. Donnelly, K. L., C. I. Smith, S. J. Schwarzenberg, J. Jessurun, M. D. Boldt, and E. J. Parks. 2005. Sources of fatty acids stored in liver and secreted via lipoproteins in patients with nonalcoholic fatty liver disease. *J. Clin. Invest.* **115:** 1343–1351.
10. Soukas, A., P. Cohen, N. D. Socci, and J. M. Friedman. 2000. Leptin-specific patterns of gene expression in white adipose tissue. *Genes Dev.* **14:** 963–980.

11. Cohen, P., M. Miyazaki, N. D. Socci, A. Hagge-Greenberg, W. Liedtke, A. A. Soukas, R. Sharma, L. C. Hudgins, J. M. Ntambi, and J. M. Friedman. 2002. Role for stearoyl-CoA desaturase-1 in leptin-mediated weight loss. *Science.* **297:** 240–243.
12. Lin, J., R. Yang, P. T. Tarr, P-H. Wu, C. Handschin, S. Li, W. Yang, L. Pei, M. Uldry, P. Tontonoz, et al. 2005. Hyperlipidemic effects of dietary saturated fats mediated through PGC-1[beta] coactivation of SREBP. *Cell.* **120:** 261–273.
13. Jiang, L., Q. Wang, Y. Yu, F. Zhao, P. Huang, R. Zeng, R. Z. Qi, W. Li, and Y. Liu. 2009. Leptin contributes to the adaptive responses of mice to high-fat diet intake through suppressing the lipogenic pathway. *PLoS ONE.* **4:** e6884.
14. Ntambi, J. M., M. Miyazaki, J. P. Stoehr, H. Lan, C. M. Kendziorski, B. S. Yandell, Y. Song, P. Cohen, J. M. Friedman, and A. D. Attie. 2002. Loss of stearoyl-CoA desaturase-1 function protects mice against adiposity. *Proc. Natl. Acad. Sci. USA.* **99:** 11482–11486.
15. Abu-Elheiga, L., W. Oh, P. Kordari, and S. J. Wakil. 2003. Acetyl-CoA carboxylase 2 mutant mice are protected against obesity and diabetes induced by high-fat/high-carbohydrate diets. *Proc. Natl. Acad. Sci. USA.* **100:** 10207–10212.
16. Jiang, G., Z. Li, F. Liu, K. Ellsworth, Q. Dallas-Yang, M. Wu, J. Ronan, C. Esau, C. Murphy, D. Szalkowski, et al. 2005. Prevention of obesity in mice by antisense oligonucleotide inhibitors of stearoyl-CoA desaturase-1. *J. Clin. Invest.* **115:** 1030–1038.
17. Gutierrez-Juarez, R., A. Pocai, C. Mulas, H. Ono, S. Bhanot, B. P. Monia, and L. Rossetti. 2006. Critical role of stearoyl-CoA desaturase-1 (SCD1) in the onset of diet-induced hepatic insulin resistance. *J. Clin. Invest.* **116:** 1686–1695.
18. Savage, D. B., C. S. Choi, V. T. Samuel, Z. X. Liu, D. Zhang, A. Wang, X. M. Zhang, G. W. Cline, X. X. Yu, J. G. Geisler, et al. 2006. Reversal of diet-induced hepatic steatosis and hepatic insulin resistance by antisense oligonucleotide inhibitors of acetyl-CoA carboxylases 1 and 2. *J. Clin. Invest.* **116:** 817–824.
19. Miyazaki, M., M. T. Flowers, H. Sampath, K. Chu, C. Otzelberger, X. Liu, and J. M. Ntambi. 2007. Hepatic stearoyl-CoA desaturase-1 deficiency protects mice from carbohydrate-induced adiposity and hepatic steatosis. *Cell Metab.* **6:** 484–496.
20. Sampath, H., M. Miyazaki, A. Dobrzyn, and J. M. Ntambi. 2007. Stearoyl-CoA desaturase-1 mediates the pro-lipogenic effects of dietary saturated fat. *J. Biol. Chem.* **282:** 2483–2493.
21. Mao, J., F. J. DeMayo, H. Li, L. Abu-Elheiga, Z. Gu, T. E. Shaikenov, P. Kordari, S. S. Chirala, W. C. Heird, and S. J. Wakil. 2006. Liver-specific deletion of acetyl-CoA carboxylase 1 reduces hepatic triglyceride accumulation without affecting glucose homeostasis. *Proc. Natl. Acad. Sci. USA.* **103:** 8552–8557.
22. Chakravarthy, M. V., Z. Pan, Y. Zhu, K. Tordjman, J. G. Schneider, T. Coleman, J. Turk, and C. F. Semenkovich. 2005. "New" hepatic fat activates PPARalpha to maintain glucose, lipid, and cholesterol homeostasis. *Cell Metab.* **1:** 309–322.
23. Fukuda, H., A. Katsurada, and N. Iritani. 1992. Effects of nutrients and hormones on gene expression of ATP citrate-lyase in rat liver. *Eur. J. Biochem.* **209:** 217–222.
24. Beigneux, A. P., C. Kosinski, B. Gavino, J. D. Horton, W. C. Skarnes, and S. G. Young. 2004. ATP-citrate lyase deficiency in the mouse. *J. Biol. Chem.* **279:** 9557–9564.
25. Bauer, D. E., G. Hatzivassiliou, F. Zhao, C. Andreadis, and C. B. Thompson. 2005. ATP citrate lyase is an important component of cell growth and transformation. *Oncogene.* **24:** 6314–6322.
26. Hatzivassiliou, G., F. Zhao, D. E. Bauer, C. Andreadis, A. N. Shaw, D. Dhanak, S. R. Hingorani, D. A. Tuveson, and C. B. Thompson. 2005. ATP citrate lyase inhibition can suppress tumor cell growth. *Cancer Cell.* **8:** 311–321.
27. Migita, T., T. Narita, K. Nomura, E. Miyagi, F. Inazuka, M. Matsuura, M. Ushijima, T. Mashima, H. Seimiya, Y. Satoh, et al. 2008. ATP citrate lyase: activation and therapeutic implications in non-small cell lung cancer. *Cancer Res.* **68:** 8547–8554.
28. Pearce, N. J., J. W. Yates, T. A. Berkhout, B. Jackson, D. Tew, H. Boyd, P. Camilleri, P. Sweeney, A. D. Gribble, A. Shaw, et al. 1998. The role of ATP citrate-lyase in the metabolic regulation of plasma lipids. Hypolipidaemic effects of SB-204990, a lactone prodrug of the potent ATP citrate-lyase inhibitor SB-201076. *Biochem. J.* **334:** 113–119.
29. Preuss, H. G., C. V. Rao, R. Garis, J. D. Bramble, S. E. Ohia, M. Bagchi, and D. Bagchi. 2004. An overview of the safety and efficacy of a novel, natural(-)-hydroxycitric acid extract (HCA-SX) for weight management. *J. Med.* **35:** 33–48.
30. Li, J. J., H. Wang, J. A. Tino, J. A. Robl, T. F. Herpin, R. M. Lawrence, S. Biller, H. Jamil, R. Ponticiello, L. Chen, et al. 2007. 2-Hydroxy-N-arylbenzenesulfonamides as ATP-citrate lyase inhibitors. *Bioorg. Med. Chem. Lett.* **17:** 3208–3211.
31. Kornacker, M. S., and J. M. Lowenstein. 1965. Citrate and the conversion of carbohydrate into fat. The activities of citrate-cleavage enzyme and acetate thiokinase in livers of starved and re-fed rats. *Biochem. J.* **94:** 209–215.
32. Wang, Q., L. Jiang, J. Wang, S. Li, Y. Yu, J. You, R. Zeng, X. Gao, L. Rui, W. Li, et al. 2009. Abrogation of hepatic ATP-citrate lyase protects against fatty liver and ameliorates hyperglycemia in leptin receptor-deficient mice. *Hepatology.* **49:** 1166–1175.
33. Sheaff, R. C., H. M. Su, L. A. Keswick, and J. T. Brenna. 1995. Conversion of alpha-linolenate to docosahexaenoate is not depressed by high dietary levels of linoleate in young rats: tracer evidence using high precision mass spectrometry. *J. Lipid Res.* **36:** 998–1008.
34. Lam, T. K. T., R. Gutierrez-Juarez, A. Pocai, S. Bhanot, P. Tso, G. J. Schwartz, and L. Rossetti. 2007. Brain glucose metabolism controls the hepatic secretion of triglyceride-rich lipoproteins. *Nat. Med.* **13:** 171–180.
35. Nakamuta, M., B. H. Chang, E. Zsigmond, K. Kobayashi, H. Lei, B. Y. Ishida, K. Oka, E. Li, and L. Chan. 1996. Complete phenotypic characterization of apobec-1 knockout mice with a wild-type genetic background and a human apolipoprotein B transgenic background, and restoration of apolipoprotein B mRNA editing by somatic gene transfer of Apobec-1. *J. Biol. Chem.* **271:** 25981–25988.
36. Davidson, N. O., and G. S. Shelness. 2000. Apolipoprotein B: mRNA editing, lipoprotein assembly, and presecretory degradation. *Annu. Rev. Nutr.* **20:** 169–193.
37. Hirano, K., S. G. Young, R. V. Farese, Jr., J. Ng, E. Sande, C. Warburton, L. M. Powell-Braxton, and N. O. Davidson. 1996. Targeted disruption of the mouse apobec-1 gene abolishes apolipoprotein B mRNA editing and eliminates apolipoprotein B48. *J. Biol. Chem.* **271:** 9887–9890.
38. Cao, H., K. Gerhold, J. R. Mayers, M. M. Wiest, S. M. Watkins, and G. S. Hotamisligil. 2008. Identification of a lipokine, a lipid hormone linking adipose tissue to systemic metabolism. *Cell.* **134:** 933–944.
39. Miyazaki, M., Y-C. Kim, and J. M. Ntambi. 2001. A lipogenic diet in mice with a disruption of the stearoyl-CoA desaturase 1 gene reveals a stringent requirement of endogenous monounsaturated fatty acids for triglyceride synthesis. *J. Lipid Res.* **42:** 1018–1024.
40. Sowden, M. P., N. Ballatori, K. L. Jensen, L. H. Reed, and H. C. Smith. 2002. The editosome for cytidine to uridine mRNA editing has a native complexity of 27S: identification of intracellular domains containing active and inactive editing factors. *J. Cell Sci.* **115:** 1027–1039.
41. Wellen, K. E., G. Hatzivassiliou, U. M. Sachdeva, T. V. Bui, J. R. Cross, and C. B. Thompson. 2009. ATP-citrate lyase links cellular metabolism to histone acetylation. *Science.* **324:** 1076–1080.
42. Lerin, C., J. T. Rodgers, D. E. Kalume, S. H. Kim, A. Pandey, and P. Puigserver. 2006. GCN5 acetyltransferase complex controls glucose metabolism through transcriptional repression of PGC-1alpha. *Cell Metab.* **3:** 429–438.
43. Li, X., S. Zhang, G. Blander, J. G. Tse, M. Krieger, and L. Guarente. 2007. SIRT1 deacetylates and positively regulates the nuclear receptor LXR. *Mol. Cell.* **28:** 91–106.
44. Kelly, T. J., C. Lerin, W. Haas, S. P. Gygi, and P. Puigserver. 2009. GCN5-mediated transcriptional control of the metabolic coactivator PGC-1beta through lysine acetylation. *J. Biol. Chem.* **284:** 19945–19952.